



# SIMULATION AND EXPERIMENTAL STUDY OF PLANAR SLOW-WAVE STRUCTURES ON DIELECTRIC SUBSTRATES FOR MICROFABRICATED TRAVELING-WAVE TUBES

R.A. Torgashov<sup>1,2</sup>, N.M. Ryskin<sup>1,2</sup>, A.V. Starodubov<sup>2</sup>, G. Ulisse<sup>3</sup>, V. Krozer<sup>3</sup>,  
A.M. Pavlov<sup>2</sup>, V.V. Galushka<sup>2</sup>, A.A. Serdobintsev<sup>2</sup>, I.O. Kozhevnikov<sup>2</sup>, A.G. Rozhnev<sup>1,2</sup>

<sup>1</sup>*Saratov Branch, Kotel'nikov Institute of Radio Engineering and Electronics RAS,*

<sup>2</sup>*Saratov State University,*

<sup>3</sup>*Goethe University Frankfurt, Physics Institute*

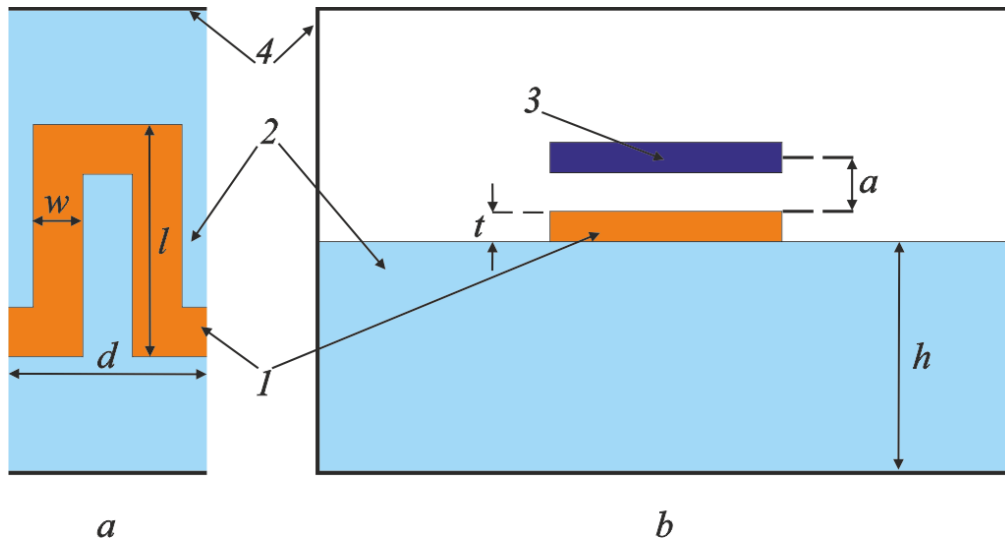
E-mail: [torgashovra@gmail.com](mailto:torgashovra@gmail.com)

7th ITG International Vacuum Electronics Workshop (IVEW) 2020 and  
13th International Vacuum Electron Sources Conference (IVeSC) 2020  
26-29 May 2020

# Introduction

- Microfabricated TWT and BWO are in great interest for application in high-speed communication, radar, security and military systems, electronic warfare, etc.
- With increasing of operating frequency of TWT dimension parameters of SWSs are decrease.
- Typical helix-based SWSs are limited by 60 GHz.
- New techniques of microfabrication of SWS are necessary.
- New types of SWSs are needed.
- Planar SWS on dielectric substrates can show high slow-wave factor (5-7) and allow low-voltage operation

# Meander-line Slow-wave structure

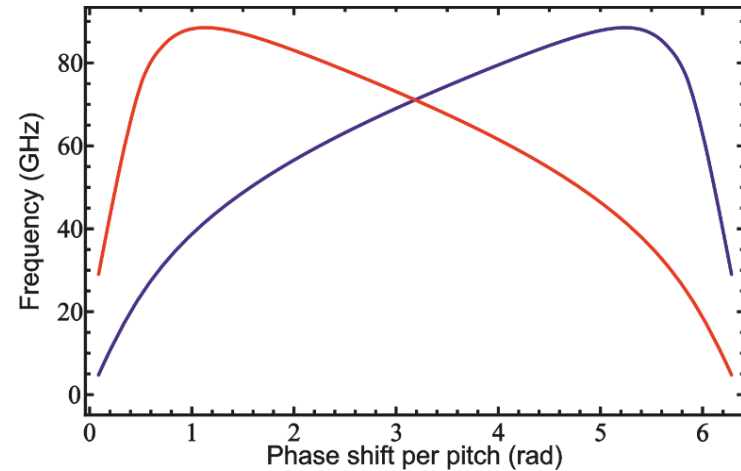


1 – Conducting line, 2 – dielectric substrate,  
3 – Electron beam, 4 - Waveguide

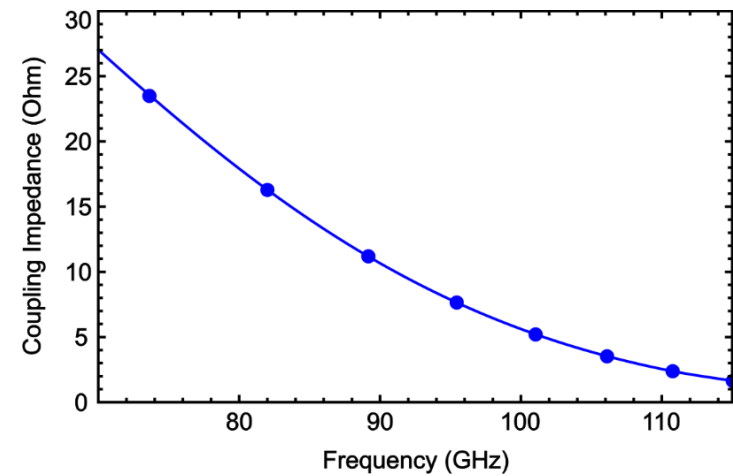
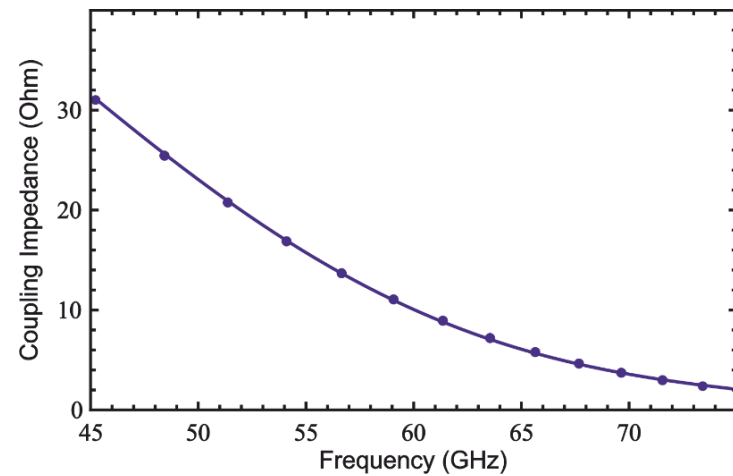
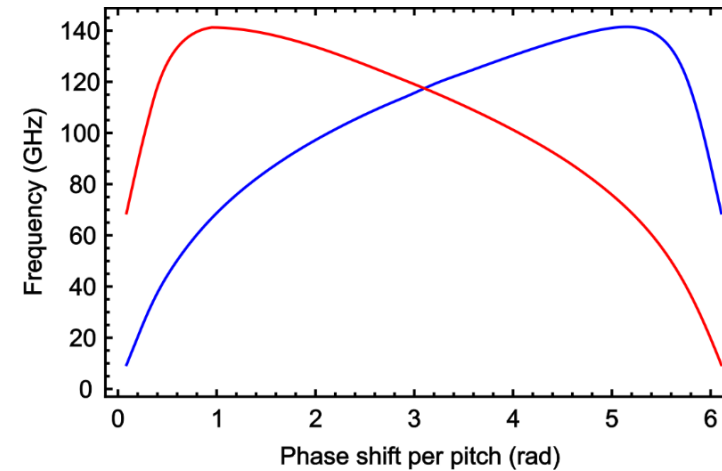
Parameter	V-band	W-band
SWS period, $d$ (um)	200	130
Pin length, $l$ (um)	650	450
Strip width, $s$ (um)	50	32.5
Slit width, $w$ (um)	50	32.5
Metallized strip thickness, $t$ (um)	10	10
Substrate thickness, $h$ (um)	500	500
Waveguide cross section (mm)	3.6×1.8	2.4×1.2

# Results of 3D Simulation

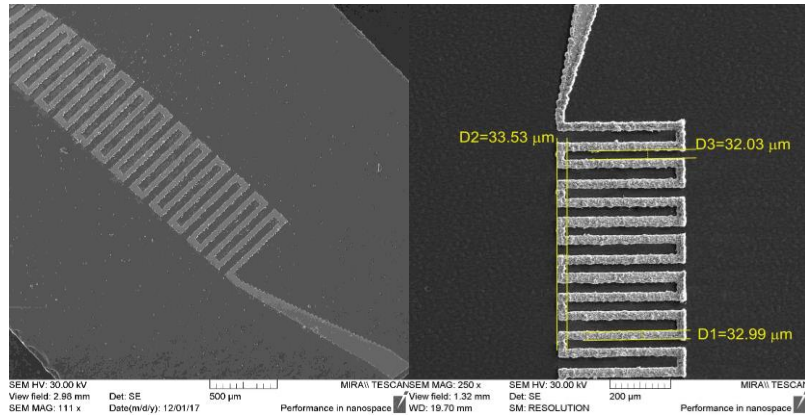
V-band



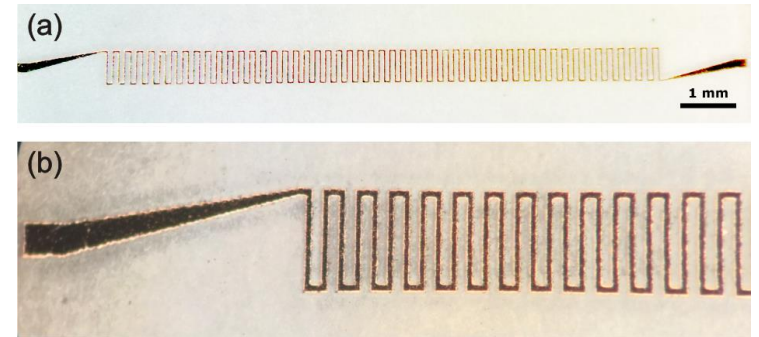
W-band



# Microfabrication of Meander SWSs



SEM image of a fabricated V- and W-band SWSs



Optical microscopy image of the meander V-band SWS (a) and its enlarged fragment (b).

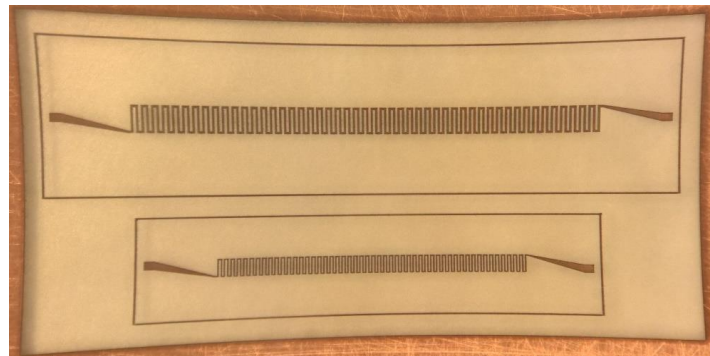


Photo of the V- and W-band meander SWS samples

# Experimental measurements and comparison with 3D simulation

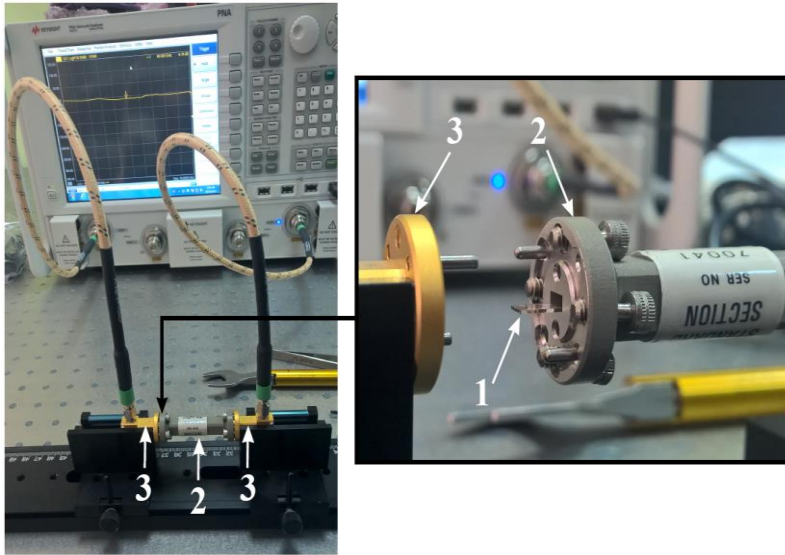
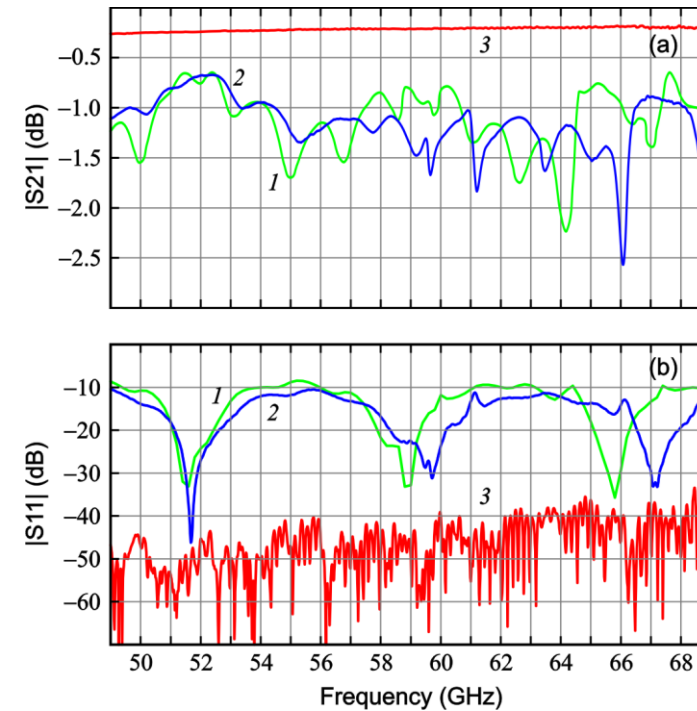
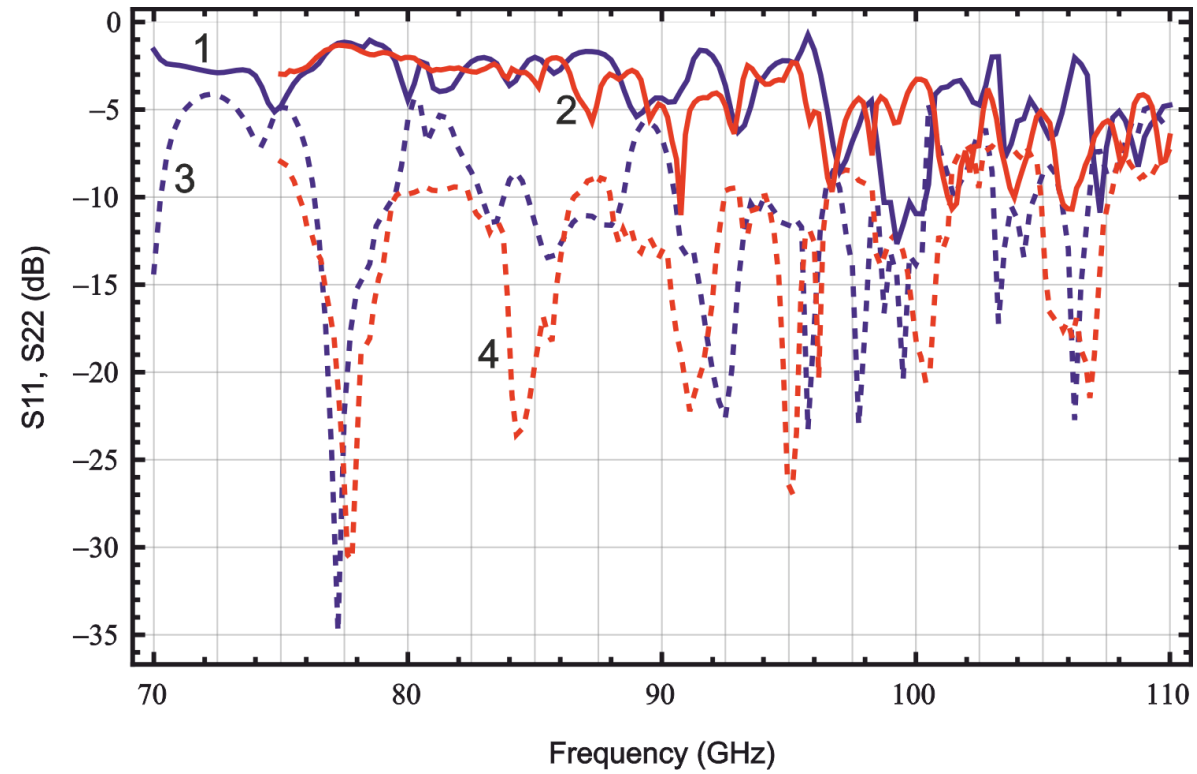


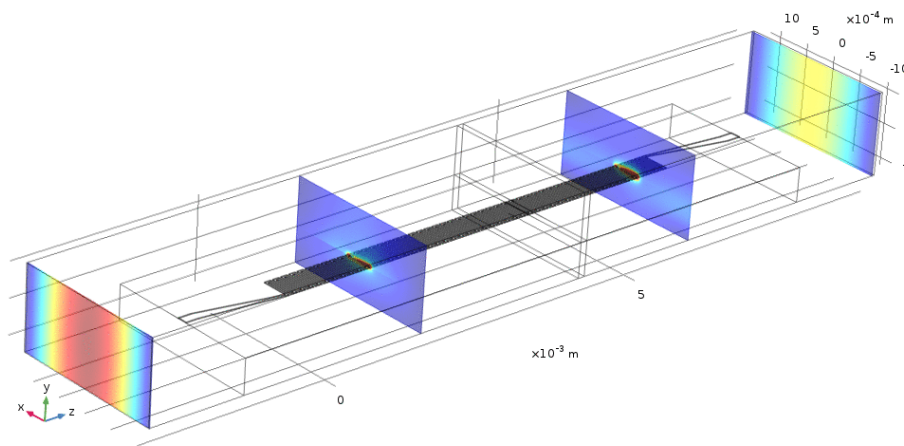
Photo of experimental setup: 1 – studied sample of SWS; 2 – standard straight WR-15 waveguide section with 5-cm length; 3 – waveguide to coax adapters.



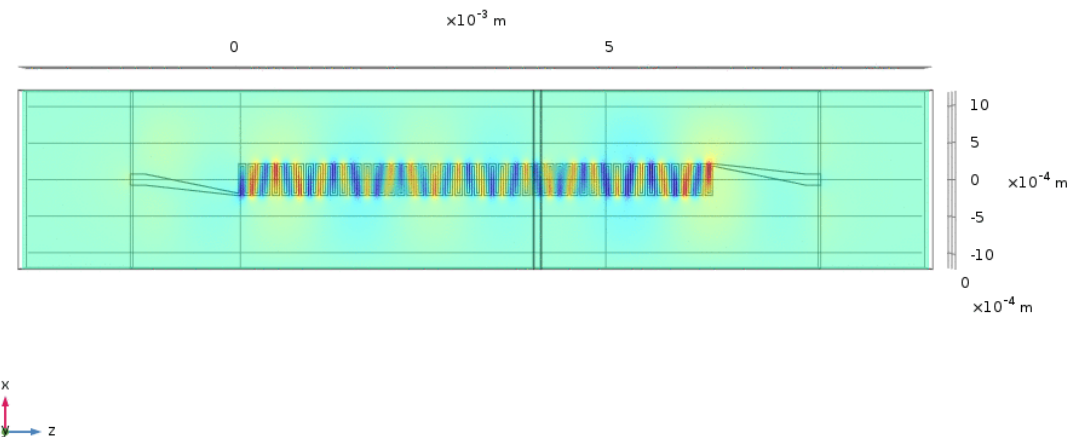
Transmission loss (a) and reflection loss (b) of the V-band meander SWS. (1) – calculations, (2) – measurements, (3) – empty waveguide (measured).



Transmission loss (1,2) and reflection loss (3,4) of the W-band meander SWS. (1,3) – calculations, (2,4) – measurements



Transverse patterns of the electric field in different points along the SWS at 60 GHz (COMSOL simulations).

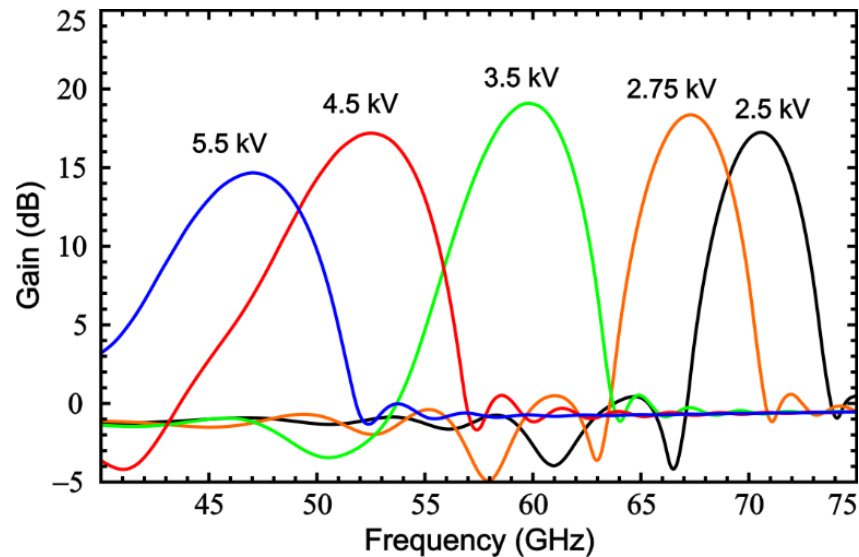


$E_z$ -field distribution at beam height of W-band meander SWS (COMSOL simulation)

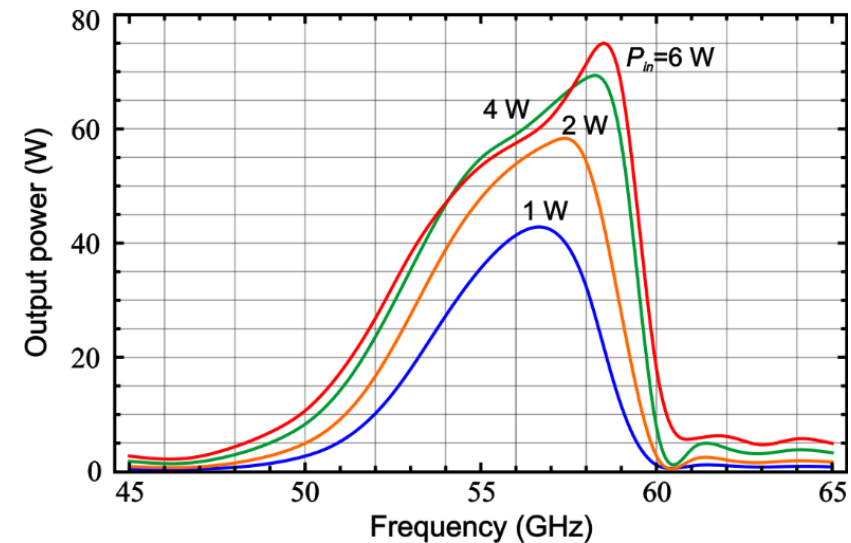
This Figure clearly demonstrates transformation of the  $TE_{10}$  waveguide mode into surface mode of the SWS. Reverse transformation is observed at the right end of the structure with losses.



# Gain simulation of the sheet-beam V-band TWT with meander SWS

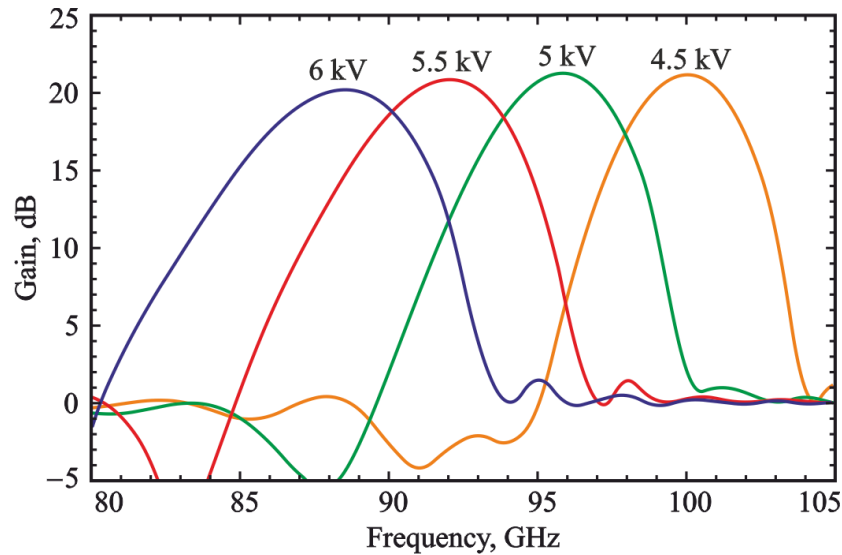


Small-signal gain of the V-band TWT versus frequency for different values of beam voltage.  $650 \times 50 \text{ } \mu\text{m}^2$  sheet beam with  $I_0 = 100 \text{ mA}$  current, SWS length  $l = 1 \text{ cm}$  (50 pitches).

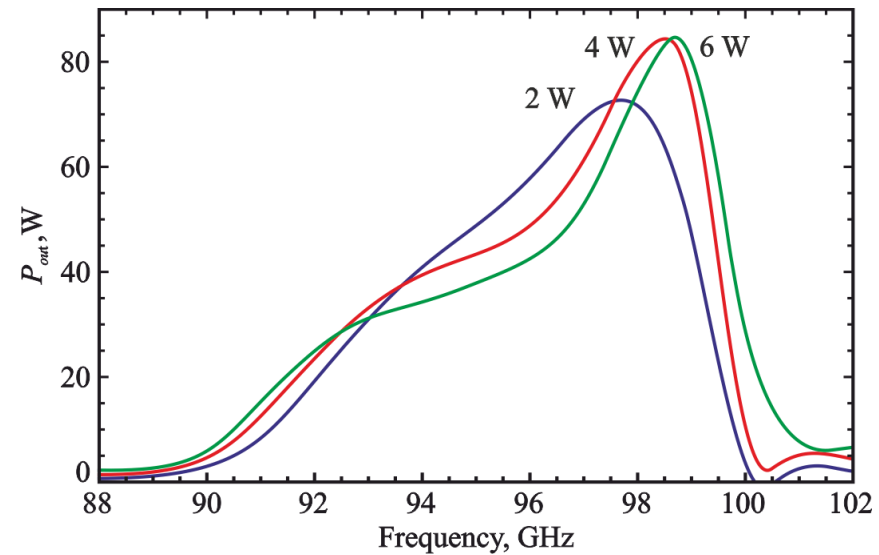


Output power versus frequency for different values of input power.  $V_0 = 4 \text{ kV}$ .

# Gain simulation of the sheet-beam W-band TWT with meander SWS

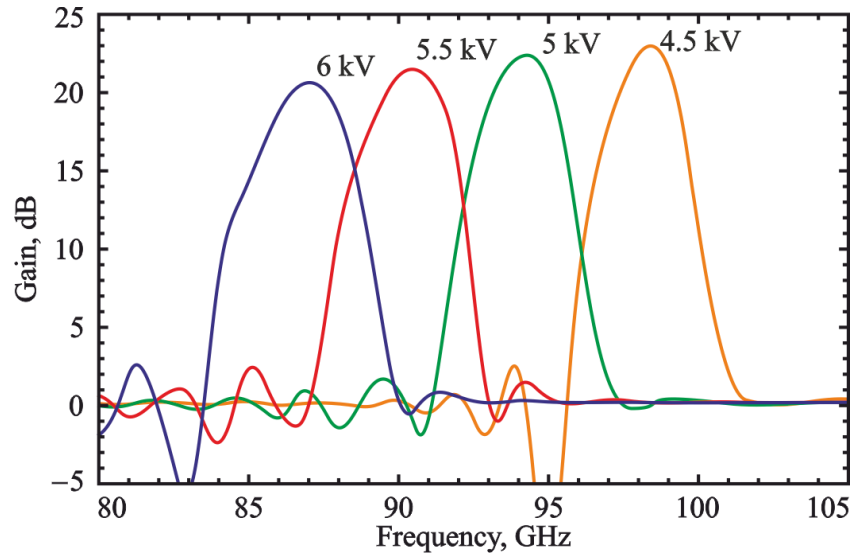


Small-signal gain of the W-band TWT versus frequency for different values of beam voltage. 450×50  $\mu\text{m}^2$  sheet beam with  $I_0 = 100\text{mA}$  current, SWS length  $l = 1\text{ cm}$  (77 pitches).

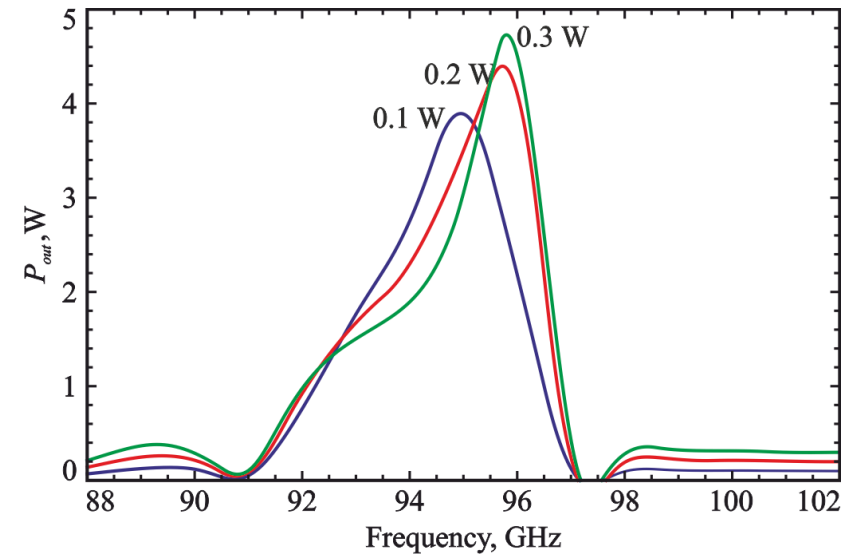


Output power versus frequency for different values of input power.  $V_0 = 5\text{ kV}$ .

The average current density is approximately 465 A /  $\text{cm}^2$  at beam current of the 100 mA. Although this value is very high, there are examples of successful focusing and transporting sheet beams with such current density over distances of several centimeters.



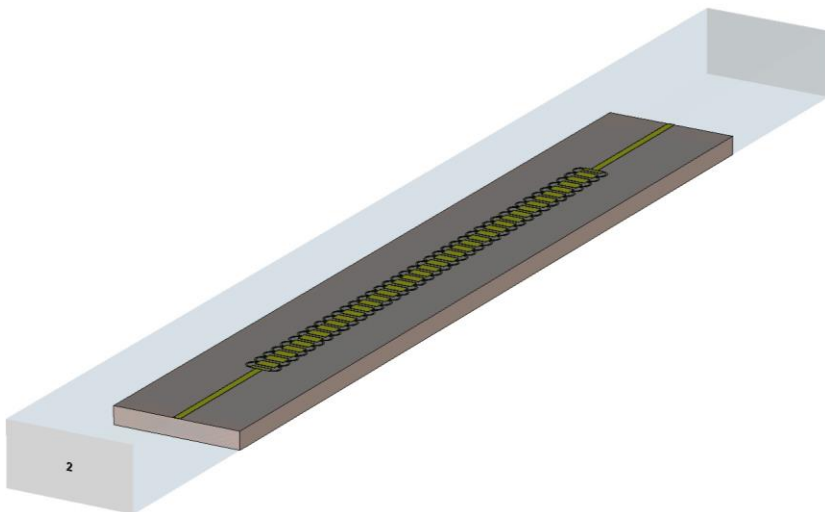
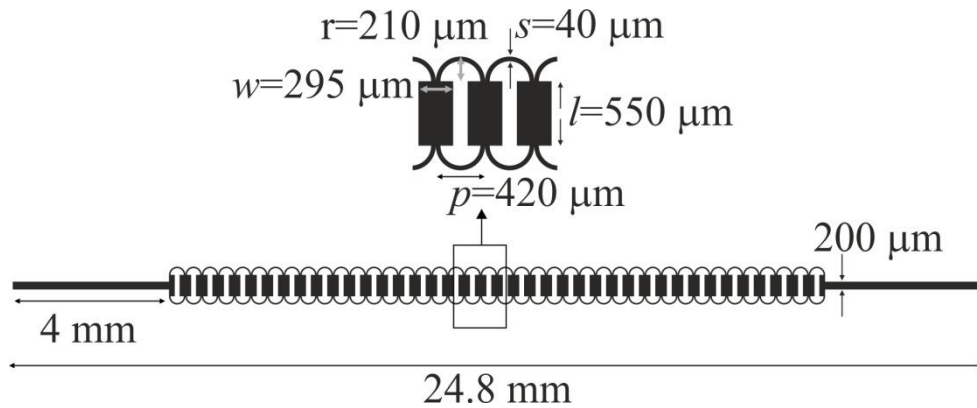
Small-signal gain of the W-band TWT versus frequency for different values of beam voltage.  $450 \times 50 \text{ } \mu\text{m}^2$  sheet beam with  $I_0 = 10 \text{ mA}$  current, SWS length  $l = 2 \text{ cm}$  (155 pitches).



Output power versus frequency for different values of input power.  $V_0 = 5 \text{ kV}$ .

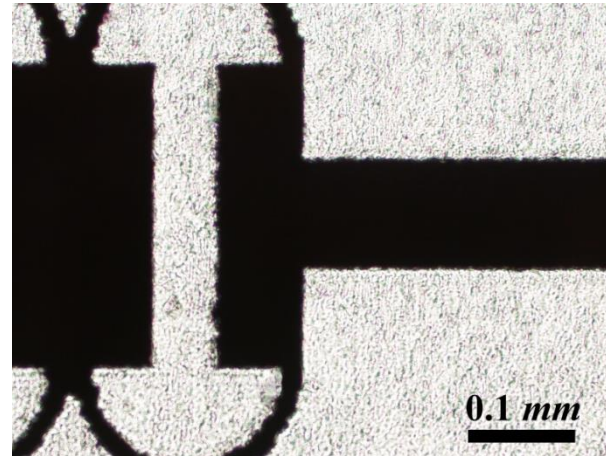
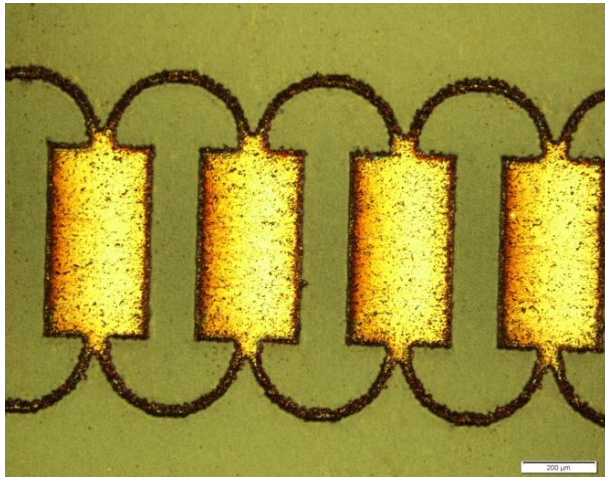
The case of such values of the beam current corresponds to the case of using an electron gun with field emission. Such beams are easier to transport over larger distances.

# V-band Ring-shaped SWS on dielectric substrate

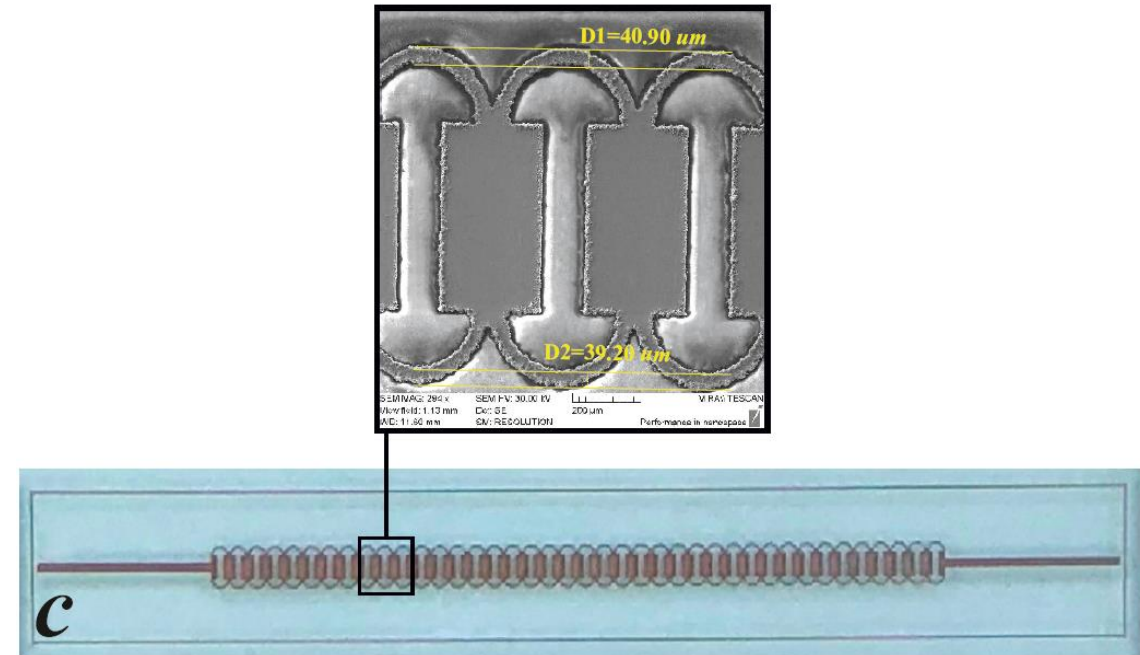


Substrate material	Quartz
Slow wave structure material	Copper
SWS period, $d$ ( $\mu\text{m}$ )	420
Metallized strip thickness, $t$ ( $\mu\text{m}$ )	5
Substrate thickness, $h$ ( $\mu\text{m}$ )	500

# Microfabrication of V-band Ring-shaped SWSs

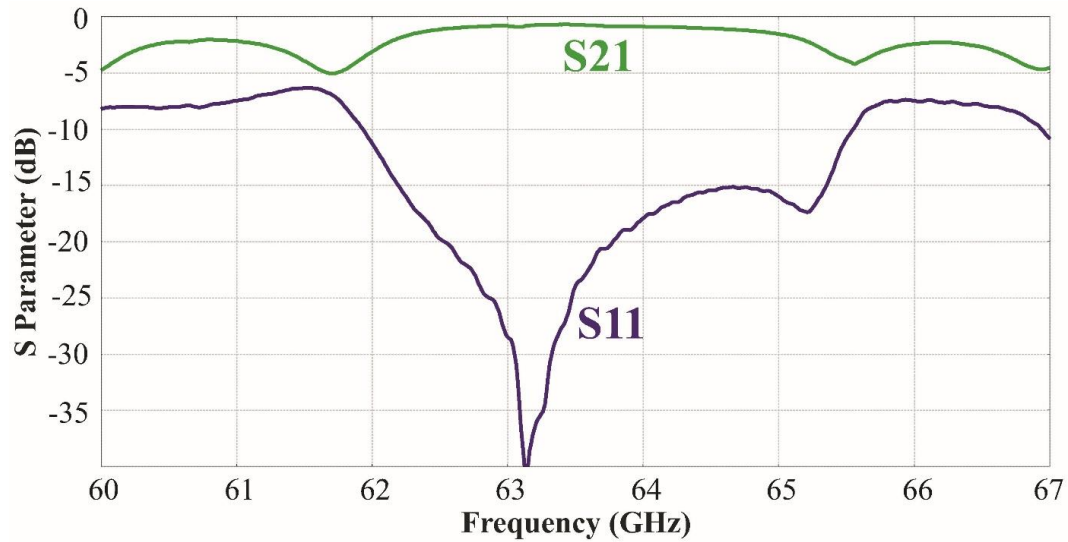


Optical microscopy images of the ring-shaped V-band SWS

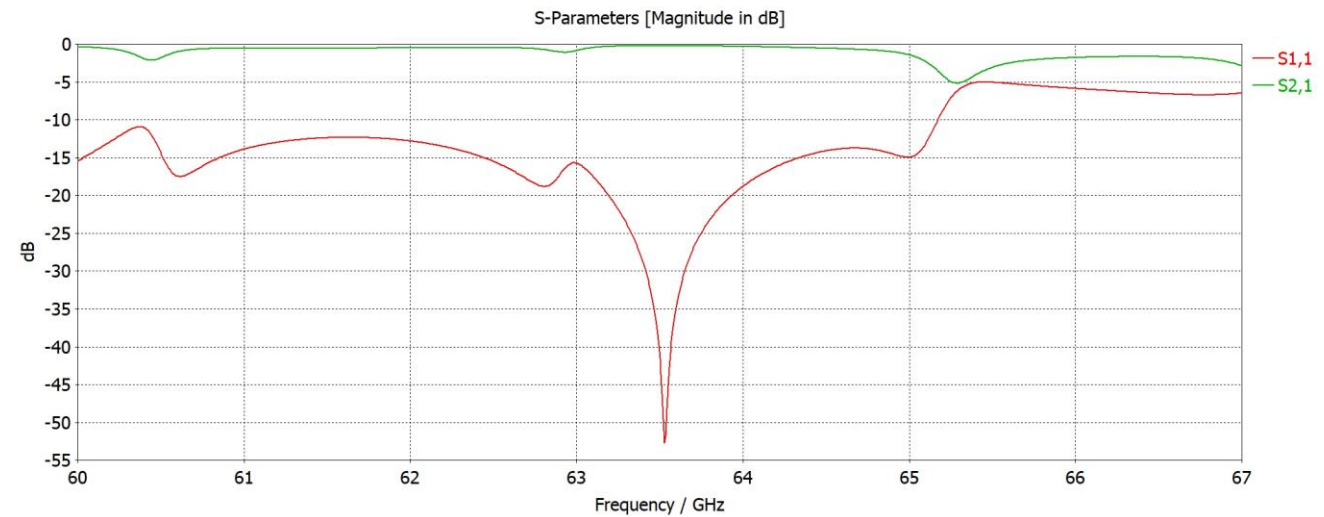


SEMs and photo of ring-shaped V-band SWS

# Experimental measurements and comparison with 3D simulation

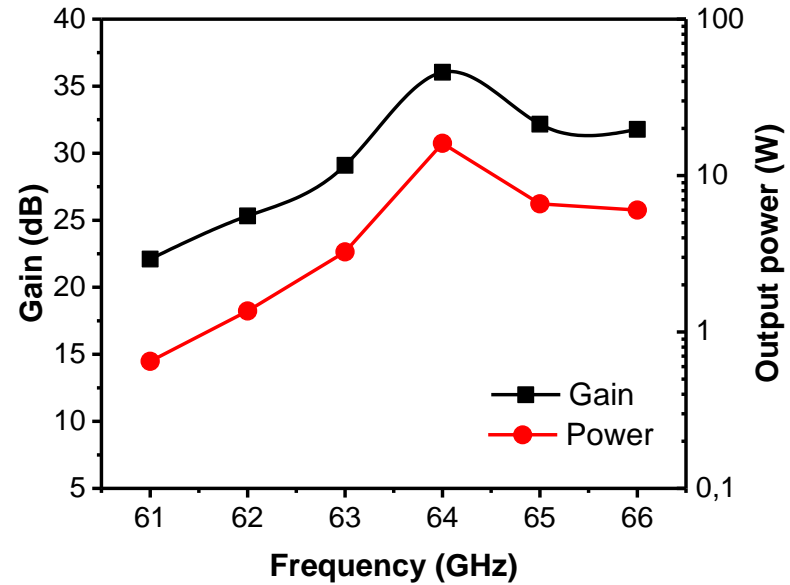


Experimental measurements



Results of CST simulation

# 3D PIC-simulations



Parameter	Value
Electron Energy	16 keV
Beam Current	50 mA
Magnetic Field	0.35 T
Input Power	4 mW
Copper conductivity	$2.25 \cdot 10^7$ S/m

# Conclusions

- Two types of SWS for V- and W-band TWT are presented.
- The planar SWS was realized with a technology, based on magnetron sputtering and laser ablation methods. This method is cheaper and faster than classic microfabrication technologies.
- Measured S-parameters show good agreement with the numerical results. Transition losses are less than -10 dB and reflection losses are better than -5 dB.
- Main output characteristics were obtained using 1D-numerical simulation and 3D PIC-simulation. Gain coefficient can reach values up to 27 dB and output power can reach 80 W.



# Thank You for your attention!

This work is supported by Russian Foundation for Basic Research (grant # 20-57-12001) and DFG (grant # 430109039).

G.U. and V.K. acknowledge partial financial support from the EU project ULTRAWAVE.

E-mail: [torgashovra@gmail.com](mailto:torgashovra@gmail.com)